Improved method for estimating the minimum length of modal filters fabricated for stellar interferometry

Sonali Dasgupta[1*], N.G.R. Broderick[1], David J. Richardson[1], Tomer Lewi[2] and Abraham Katzir[2]

[1]*Optoelectronics Research Center, University of Southampton, SO17 1BJ United Kingdom*

[2]*School of Physics and Astronomy, Tel- Aviv University, Tel Aviv 69978, Israel*

[*]*Corresponding author:*
sxd@orc.soton.ac.uk

Abstract: We present an improved theoretical model to estimate the minimum fiber length required for achieving a desired degree of wavefront filtering in stellar interferometry. The proposed model is based on modal analysis of the fiber and is compared with numerical results obtained through the beam propagation method as well as with reported experimental observations. We also study the effect of introducing a spatial filter at the output end of the fiber and show that the required fiber length can be reduced significantly by introducing a circular aperture of optimum radius after the fiber.

OCIS codes: (350.1260) Astronomical optics; (060.2390) Fiber optics, infrared; (350.2450) Filters, absorption

References and links

1. http://exoplanets.org/planets.html.
2. http://www.esa.int/esaSC/SEMYZF9YFDD_index_0.html.
3. R.N.Bracewell, "Detecting nonsolar planets by spinning infrared interferometer," Nature **274**, 780 – 781 (1978).
4. K. Wallace, G. Hardy, and E. Serabyn, "Deep and stable interferometric nulling of broadband light with implications for observing planets around nearby stars," Nature **406**, 700–702 (2000).
5. J. R. P. Angel and N. J. Woolf, "An Imaging Nulling Interferometer to Study Extrasolar Planets," The Astrophys. J. **475**, 373–379 (1997), http://www.journals.uchicago.edu/doi/abs/10.1086/303529.
6. www.esa.int/esaSC/120382_index_0_m.html.
7. http://planetquest.jpl.nasa.gov/TPF/tpf_index.cfm.
8. E. Serabyn, S. Martin, and G. Hardy, "Progress toward space-based nulling interferometry: comparison of null stabilization approaches," Aerospace Conference, 2001, IEEE Proceedings. **4**, 4/2027–4/2036 (2001).
9. B. Mennesson, M. Ollivier, and C. Ruilier, "Use of single-mode waveguides to correct the optical defects of a nulling interferometer," J. Opt. Soc. Am. A **19**, 596–602 (2002), http://josaa.osa.org/abstract.cfm?URI=josaa-19-3-596.
10. M. Ollivier and J.-M. Mariotti, "Improvement in the rejection rate of a nulling interferometer by spatial filtering," Appl. Opt. **36**, 5340–5346 (1997), http://ao.osa.org/abstract.cfm?URI=ao-36-22-5340.
11. J. Flanagan and D. Richardson, "Microstructured fibres for broadband wavefront filtering in the mid-IR," Opt. Express **14**, 11773–11786 (2006).
12. O. Wallner and W. Leeb, "Minimum length of a single-mode fibre spatial filter," JOSA A **19**, 2445–2448 (2002).
13. J. C. Corbett and J. R. Allington-Smith, "Coupling starlight into single-mode photonic crystal fiber using a field lens," Opt. Express **13**, 6527–6540 (2005).
14. T. Lewi, S. Shalem, A. Tsun, and A. Katzir, "Silver halide single-mode fibers with improved properties in the infrared," Appl. Phys. Lett. **91**, 2511,112–1 – 2511,112–3 (2007).

#103283 - $15.00 USD Received 27 Oct 2008; revised 24 Dec 2008; accepted 18 Jan 2009; published 30 Jan 2009

15. A. Ksendzov, O. Lay, S. Martin, J. S. Sanghera, L. E. Busse, W. H. Kim, P. C. Pureza, V. Q. Nguyen, and I. D. Aggarwal, "Characterization of mid-infrared single mode fibers as modal filters," Appl. Opt. **46**, 7957–7962 (2007).
16. P. Houizot, C. Boussard-Plédel, A. J. Faber, L. K. Cheng, B. Bureau, P. A. V. Nijnatten, W. L. M. Gielesen, J. P. do Carmo, and J. Lucas, "Infrared single mode chalcogenide glass fiber for space," Opt. Express **15**, 12,529–12,538 (2007), http://www.opticsexpress.org/abstract.cfm?URI=oe-15-19-12529.
17. W. Klaus, and W. R. Leeb, "Transient fields in the input coupling region of optical single-mode waveguides," Opt. Express **15**, 11808–11826(2007), http://www.opticsexpress.org/abstract.cfm?URI=oe-15-19-11808.
18. A. W. Snyder and J.D.Love, *Optical waveguide theory* ((Chapman/Kluwer, 1983/2000).
19. G. Huss, P. Leproux, F. Reynaud, and V. Doya, "Spatial filtering efficiency of single-mode optical fibers for stellar interferometry applications: phenomenological and numerical study," Opt. Commun. **244**, 209–217 (2005).
20. A. Ksendzov, T. Lewi, O. P. L. S. R. Martin, R. O. Gappinger, P. R. Lawson, R. D. Peters, S. Shalem, A. Tsun, and A. Katzir, "Modal filtering for midinfrared nulling interferometry using single mode silver halide fibers," Appl. Opt. **47**, 5728–5735 (2008).
21. D. Marcuse, "Radiation losses of the dominant mode in round dielectric waveguides," Bell Syst. Tech. J. **49**, 1665–1693 (1970).
22. Z. L. Wang, H. Ogura, and N. Takahashi, "Radiation and coupling of guided modes in an optical fiber with a slightly rough boundary: stochastic functional approach," J. Opt. Soc. Am. A **12**, 1489–1500 (1995).

1. Introduction

The search for extrasolar earth-like planets and extra-terrestrial life has garnered a lot of attention lately. Extrasolar planets are planets beyond the solar system that orbit around other stars and have the possibility of supporting life. To date, around 228 extrasolar planets have been identified [1]. Most of these have been detected by indirect methods like the radial velocity method and the transit method [2]. However, the indirect methods are incapable of detecting relatively smaller earth-sized planets, and providing information about their chemical composition and physical environment. Thus, it is proposed to make direct measurements of the light emitted by the planets themselves [3–5]. This has led to the launch of planet-finder projects like the DARWIN mission by the European Space Agency (ESA) [6] and the Terrestrial Planet Finder mission by the National Aeronautics and Space Administration (NASA) [7], which aim to collect light emitted by the planets directly and perform spectroscopic analysis in order to detect signs of life-supporting elements and compounds such as oxygen, water and carbon etc. However, observing extrasolar planets directly is extremely difficult because these planets usually revolve around a much brighter 'parent' star, which is typically a million times brighter than the planet (at infrared wavelengths). Thus, in order to perform spectroscopic analysis of light emitted by the planet, it is imperative to extract the faint signal emitted by the planet from the much brighter light signal emitted by the parent star [6, 7]. This involves using the nulling interferometry technique [3, 5, 8] to suppress the starlight in the signal collected by the multiple space-based telescopes. It has been reported that optical instrumentation constraints on the nulling interferometer are drastically relaxed if the wavefronts reaching the interferometer are devoid of any distortions [9, 10]. This can be achieved through wavefront (modal and spatial) filtering. Single-mode waveguides (optical fibers) are the best suited wavefront filters for this purpose [9, 11–13] since they can rectify all the spatial frequencies and a wide range of optical aberrations with minimal loss of photon flux over a wide range of wavelengths.

2. Single-mode fibers for wavefront filtering

The efficiency of a wavefront filter (optical fiber, in this case) is proportional to its capability to reject any light signal apart from the fundamental mode (FM). It is measured in terms of the ratio of power in the FM to the power in all the other leaky cladding modes at the output [12], which we define by the parameter R (rejection ratio) as follows:

#103283 - $15.00 USD Received 27 Oct 2008; revised 24 Dec 2008; accepted 18 Jan 2009; published 30 Jan 2009

$$R(L) = \frac{P_{FM}(z=L)}{P_{HOM}(z=L)} \tag{1}$$

where P_{FM} and P_{HOM} is the power in the FM and HOMs, respectively, at the output end of the fiber. Propagation is assumed along the z-direction and L is the length of the fiber. The cladding modes have effective indices lower than the refractive index of the core but greater than the refractive index of the cladding. They are leaky in nature and their field extends well into the fiber cladding. We refer to these modes as higher order modes (HOMs) or leaky cladding modes in the remaining section of the paper.

The degree of wavefront filtering ($R(L)$) that would be required to detect an Earth-sized life-supporting planet is $\sim 10^5$-10^6 (ie. 50-60dB) [6]. Since the strongest emission lines from planets usually lie in the infrared wavelength range (4-20μm), the design of single-mode fibers that can provide such an extreme level of filtering over such a broad wavelength range is a highly challenging task. The two material systems that are being investigated extensively for fabricating these fibers are silver halide [14] and chalcogenide glass [15, 16].

The single-mode fibers typically consist of a core and cladding that is surrounded by an absorption coating for achieving maximal suppression of the cladding modes [12, 14]. Ideally, the spatial distribution of the output of a single-mode fiber is independent of the input launching conditions. However, in practice, the input field excites the FM of the fiber as well as thousands of cladding modes. Thus, a certain fraction of the output power always remains in the cladding modes, which ultimately limits its filtering performance. The absorption coating on the fiber serves to increase the confinement loss of unwanted cladding modes, thereby improving the filtering capability. Longer lengths of fiber have a lower fraction of power in the cladding modes and hence, are better wavefront filters. However, deployment in space requires use of the minimum possible fiber length ($\sim$ few centimeters), thereby making it crucial to correctly estimate the minimum fiber length required to achieve the desired rejection ratio of 60dB. The minimum length depends critically on the fiber's modal characteristics and launching conditions.

A lot of research has focused on developing theoretical models to estimate the minimum fiber length [12, 14, 17]. Previously reported models [12, 14] considered the worst case scenario by assuming that the fraction of input power that is not coupled into the FM gets coupled into the HOM having the lowest loss, which is the LP_{11} mode in case of a step-index fiber with an infinitely extended cladding, resulting in the following expression for R (using Eq.1)

$$R = \frac{\eta_0 e^{-\alpha_0 L}}{(1-\eta_0)e^{-\alpha_1 L}} \tag{2}$$

where η_0 and α_0 is the coupling efficiency and confinement loss of the FM of the fiber and α_1 is the loss of the LP_{11} mode.

In this paper, we show that the model [12] is over-simplified for application to the realistic fibers used for wavefront filtering. Such fibers have a finite cladding that is surrounded by an absorption coating that may be a high-index material, such as chromium, which is used for chalcogenide fibers [16]. The finite cladding supports numerous cladding modes and the LP_{11} mode does not necessarily have the lowest loss in such structures. Moreover, the fraction of the input power that is coupled into a particular HOM depends critically on the launching conditions. Even if a particular cladding mode has very low loss, it may not be a dominant factor in deciding the filter length if its coupling efficiency is negligible. We present a model based on the modal analysis of the fiber that incorporates the effect of the coupling efficiencies along with the modal loss to estimate the filter length. We also calculate the filter length using the beam propagation method (BPM) and compare the results obtained by the two techniques. Finally, we compare the theoretical results with experimental observations made with silver halide fibers fabricated at Tel Aviv University.

#103283 - $15.00 USD Received 27 Oct 2008; revised 24 Dec 2008; accepted 18 Jan 2009; published 30 Jan 2009

3. Proposed model

3.1. Input field

In stellar interferometry (direct feed), the fiber is usually placed in the focal plane of the telescope [5]. The field exiting the telescope is in the form of an Airy disk and is fed into the single-mode fibers for wavefront filtering. The size of the Airy disk (field) is optimized to ensure optimal coupling into the single-mode fiber. The maximum overlap is provided by a diffraction limited point spread function (PSF) of the telescope aperture, on axis with no obscuration and of the appropriate scale. In the simulations presented here, we assume the input field to be an on-axis Airy disk that provides maximum overlap ($\sim$ 78%) with the FM of the fiber (described in Section 4), at the operating wavelength of 10.6μm.

3.2. Modal analysis

The power coupling efficiency (η) of the input field launched into a particular mode of an optical fiber (neglecting the effect of Fresnel reflections at the fiber facets) is proportional to the overlap integral, and is defined as [18]

$$\eta = \frac{\left|\iint_A E_{in}^* E_{op} dxdy\right|^2}{\iint_A |E_{in}|^2 dxdy \iint_A \left|E_{op}\right|^2 dxdy} \tag{3}$$

where E_{in} is the complex input field and E_{op} is the optical mode of the fiber. A is the fiber area on the $X-Y$ plane transverse to the optical axis. In the proposed model, we first calculate the confinement loss and power coupling efficiencies of the FM as well as a large number ($\approx$ 300) cladding modes of the fiber. The complex effective indices of the fiber modes are obtained by solving the full-vectorial Maxwell differential equations using the finite-element method (with the commercial software, COMSOL®). The imaginary parts of the effective indices are proportional to the confinement loss of the modes. Let η_i and α_i be the coupling efficiency and confinement loss of the i^{th} cladding mode, respectively. If we neglect inter-modal scattering, the fraction of power remaining in the various modes after a certain length of the fiber would depend on the coupling efficiency of the modes at the input and their confinement loss. This is elaborated in Fig. 1 wherein we have plotted the power carried by the various modes propagating along a fiber. The launch field is an Airy disk and the modal power at the input is normalized with respect to the coupling efficiency to that particular mode. It can readily be seen that even though modes (e,f) exhibiting loss comparable with the fundamental mode exist, they would carry a negligible fraction of the power for practical excitation conditions. Thus, modes (b,c,d) that have higher overlap with the input field are likely to be more important even though their confinement losses are higher than modes (e,f). This is in contrast to the assumptions of the previous models based on the modal confinement loss alone [12]. We assume that the fraction of power that does not get coupled into the FM (i.e. $1-\eta_0$) is distributed amongst only those cladding modes that have coupling efficiency greater than a certain threshold; we chose a threshold of 0.1% of the input field. The fractional power coupled into these modes is proportional to their overlap with the input field. Since the total power is constant, the coupling efficiency (η_i') of these cladding modes is modified as follows:

$$\sum_i^N \eta_i' = a * \sum_{i=1}^N \eta_i = 1 - \eta_0 \tag{4}$$

where a is the constant of proportionality and N is the number of modes that have coupling efficiency greater than 0.1%.

#103283 - $15.00 USD Received 27 Oct 2008; revised 24 Dec 2008; accepted 18 Jan 2009; published 30 Jan 2009

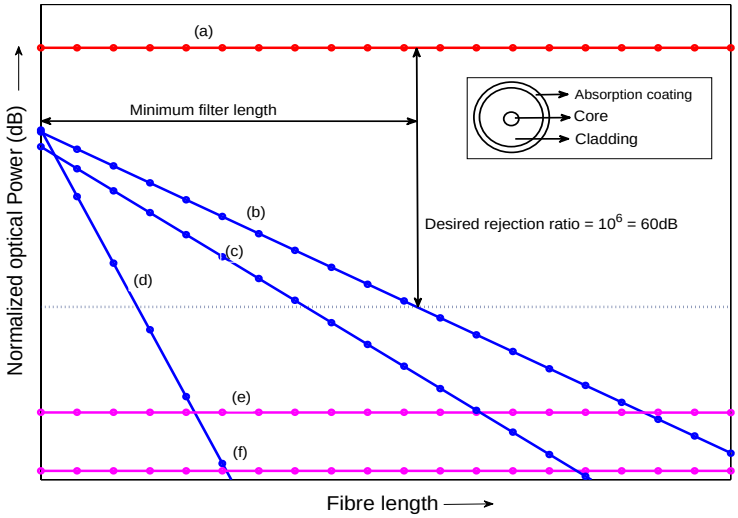

Fig. 1. Schematic representation of the modal power along the fiber length (a) FM (b-d) Modes whose overlap with the input field is $> 1\%$ (e,f) HOMs exhibiting very low confinement losses. The y-axis shows the power of the various modes such that the power is proportional to the coupling efficiency of the respective modes. The total power is assumed to be 1, which is the sum of the coupling efficiencies of all the modes. Inset: Cross-section of the fibre structure

By considering only a finite number of modes the total coupled energy is less than the actual input energy. We therefore change the weighting of all the modes equally by a factor "a" to ensure that the coupled energy equals the input energy. Since physically any light that is not coupled into the chosen modes goes into modes with higher loss, introducing the factor 'a' increases the length estimate (but only by a small amount) and so would serve to increase the rejection ratio. Equation (4) shows that a cladding mode having a higher overlap with the input field will account for a higher fraction of power in the cladding at the fiber input. Using Eq.1, $R(L)$ is now defined as

$$R(L) = \frac{\eta_0 e^{-\alpha_0 L}}{\sum_{i=1}^{N} \eta_i' e^{-\alpha_i L}} \tag{5}$$

Equation (5) is numerically solved to obtain an estimate of the minimum fiber length (L) required to achieve the desired value of R. It is important to note that we have ignored inter-modal scattering and inter-modal power transfer.

4. Results and discussion

The fiber studied in this paper is a silver halide fiber that was fabricated at Tel Aviv University [14]. It has a core radius of 25 μm and cladding radius of 350 μm. The refractive indices of the core and cladding are 2.0869 and 2.0822 respectively. A 100 μm thick absorption coating was deposited on the cladding, which exhibited a loss of $\sim$ 500 dB/m at infrared wavelengths. The absorption coating was index-matched to the cladding. The Numerical Aperture (NA) of the fiber was 0.14 at 10.6μm wavelength and its cut-off wavelength was 9.14μm. Due to the presence of the absorption layer, all the modes supported by the fiber are lossy, including the

#103283 - $15.00 USD Received 27 Oct 2008; revised 24 Dec 2008; accepted 18 Jan 2009; published 30 Jan 2009

FM. This results in complex propagation constants of the modes where the imaginary part of the propagation constant is proportional to the confinement loss of the modes. However, the loss of the FM is negligible due to its tight confinement within the core of the fiber. The cladding of the fiber supports numerous (several 100) unwanted leaky cladding modes. Fortunately, simulations showed that most of these modes exhibit very high confinement loss ($>$ 200 dB/m) and are lost within a few centimeters of propagation in the fiber. Among the modes that have losses less than 200dB/m, the fiber supported 12 cladding modes that had coupling efficiency $>$ 0.1% and are of interest according to the proposed model. Figure 2 shows the loss and coupling efficiency of these modes. Figure 3(a) shows that the intensity distribution of the incident field (Airy disk) and Fig. 3(b) shows the FM excited in the fiber, which is well-confined within the central core at 10.6μm. Substituting the loss and coupling efficiency values of the cladding modes plotted in Fig. 2 into Eq. (5) yields a minimum fiber length of $\sim$ 48cm to achieve $R = 60$dB. This length is strongly influenced by the lowest loss ($\sim$ 105dB/m) that is exhibited by these modes. We observe that most of these cladding modes have an intensity maxima at the center of the fiber, which results in the large value of the overlap. Figure 3(c) shows the transverse intensity profile of the mode that has the highest coupling efficiency with the input field. In comparison to the proposed method, the previously reported model [12] yields a filter length of almost $\sim$ 132cm for achieving the same value of R (using Eq. (2)). It is also important to note that the loss of the LP_{11} mode ($\sim$ 41dB/m) is not the lowest loss exhibited among all the cladding modes. In Fig. 3(d) we show the transverse intensity profile of the LP_{11} mode. It's coupling efficiency with the input field is theoretically zero since it is an anti-symmetric mode while the Airy disk is a symmetric field. The lowest loss exhibited amongst all the cladding modes is $\sim$ 33 dB/m. However, this mode also has a coupling efficiency $<$ 0.1%. Thus, if we consider modes with coupling efficiency $>$ 0.1%, both the LP_{11} mode and the lowest loss mode are not involved in the model for estimating the minimum filter length.

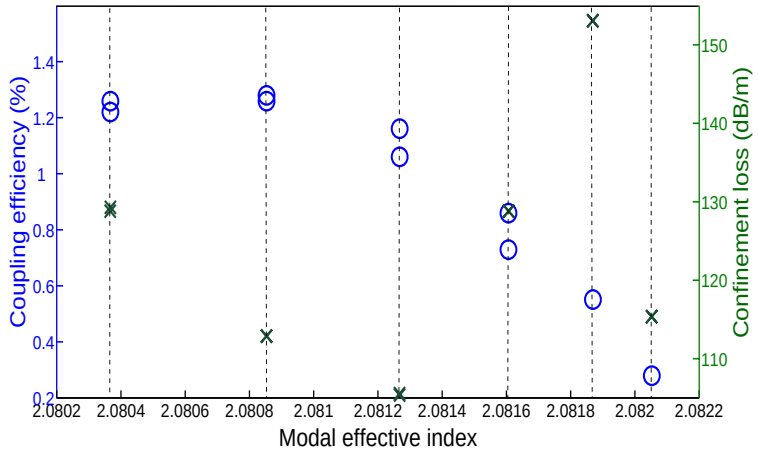

Fig. 2. Loss and coupling efficiency of the 12 cladding modes with coupling efficiency $>$ 0.1%. The circles and crosses represent the coupling efficiency and confinement loss, respectively. Note that the number of dots and crosses seem less than 12 in the figure because some of the modes are degenerate with similar values of coupling efficiency and confinement loss, and thus the dots and crosses overlap for some of the modes. Modal effective index = propagation constant of the mode / free space wave vector of light

#103283 - $15.00 USD Received 27 Oct 2008; revised 24 Dec 2008; accepted 18 Jan 2009; published 30 Jan 2009

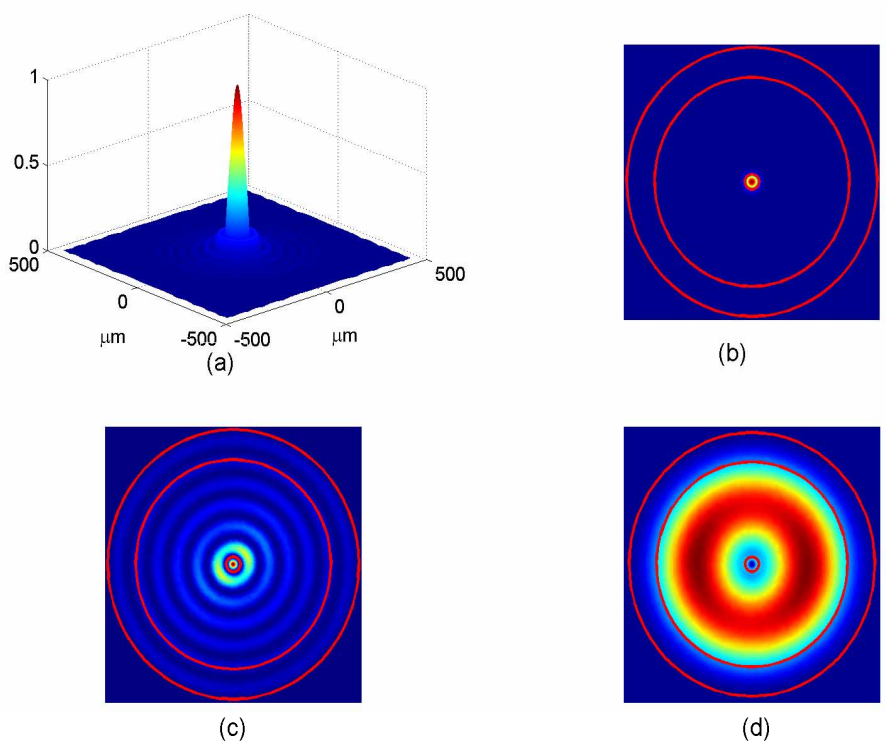

Fig. 3. Transverse intensity profile of (a) input field (Airy disk) (b) FM (c) cladding mode with highest coupling efficiency ($\approx 1.28\%$) (d) LP_{11} mode (whose overlap with the Airy disk is zero). The solid red lines in Fig. 3 (b-d) represent the fiber geometry. The innermost ring shows the core, the annular region adjacent to the core is the cladding and the outermost annular region shows the extent of the absorption coating.

4.1. Beam propagation method

In order to validate the results yielded by the proposed method, we also estimated the minimum filter length by the beam propagation method. We launched the input field (Airy disk) into a 50cm long fiber and propagated it using the commercially available software BeamPROP®. The Airy disk was optimized to provide maximum overlap (78%) with the FM at the wavelength of 10.6μm. The computational domain in the $X-Y$ plane was $\pm 456\,\mu$m. The longitudinal step size was 1μm, which was small enough to correctly model the evolution and diffraction of the optical field along the fiber [19]. We obtained field output slices every 10cm along the length of the fiber. At each of these points, the fraction of power in the FM was obtained by calculating the overlap integral of the total optical field and the FM. The overlap integral was normalized to the local optical power. $R(L)$ was subsequently obtained by using Eq.1 and assuming that all the power that is not in the FM is carried by the HOMs. Fig. 4 shows the evolution of the total power and fractional power in the FM along the length of the fiber. As the propagation distance increases, the fraction of power carried in the FM increases, thereby implying improved filtering by the fiber. For longer lengths of the fiber, the power in many of the cladding modes that extend well into the cladding is lost due to radiation and absorption by the absorptive coating, leaving only the FM and cladding modes that are localized near the core. Thus, the effect of the absorption coating reduces at longer fiber lengths and the rate of decrease of total optical

#103283 - $15.00 USD Received 27 Oct 2008; revised 24 Dec 2008; accepted 18 Jan 2009; published 30 Jan 2009

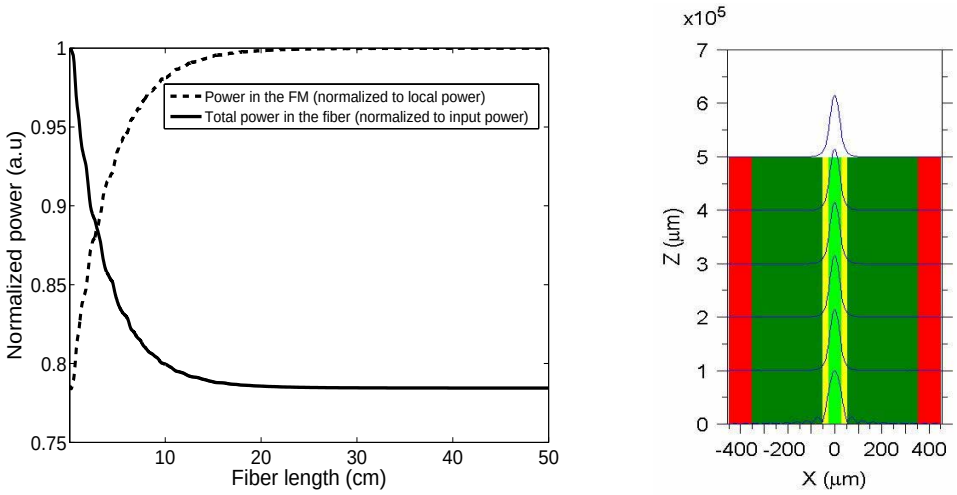

Fig. 4. Evolution of the total power (normalized to the input power) and power in the FM (normalized to the local power) along the fiber length. The right-hand side figure shows the evolution of the modal profile along the fiber length. *X* and *Z* denote the radial distance and direction of propagation, respectively. The region shaded in light green is the core of the fiber. The regions colored in yellow and dark green are the cladding, and the outermost region shaded in red is the absorption coating.

power (slope of the black solid line in Fig. 4) also reduces with fiber length. The right-hand side figure illustrates the evolution of the optical field along the fiber length. Side lobes in the modal profile that extend into the cladding can be seen very close to the input end of the fiber because the launching field is an Airy disk, and the FM profile stabilizes only after propagating through a certain length of the fiber.

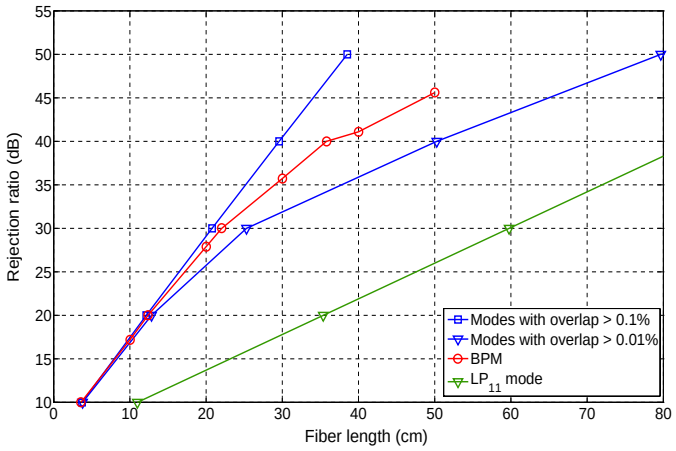

Fig. 5. Comparison of the minimum fiber length calculated by the proposed model and the BPM method

Figure 5 presents the minimum filter lengths obtained by using the model proposed in Section 3 (Eq. (5)) and the lengths obtained through the BPM method. We have plotted the lengths obtained by considering a finite number of cladding modes whose coupling efficiency with the

#103283 - $15.00 USD Received 27 Oct 2008; revised 24 Dec 2008; accepted 18 Jan 2009; published 30 Jan 2009

input field is $> 0.01\%$ and 0.1%. For comparison purposes, we have also shown the filter length predicted by the previously reported model that considers the LP_{11} mode alone [12]. It can be seen that the lengths obtained by the proposed model and BPM are in good agreement for R up to ~ 35dB. The fact that the minimum fiber length is independent of the threshold that we set on the overlap of the modes with the input field justifies our assumption that we can approximate the power distribution and propagation of all the cladding modes of the fiber by considering the propagation of just a finite number of cladding modes that have the highest overlap with the input field. However, we observe that the estimates of the filter length do not compare very well for $R > 35$dB. This can be attributed to the fact that for $R > 35$dB, the cladding modes that have coupling efficiency less than $< 0.1\%$ along with low-loss become significant, and these should also be considered for obtaining a correct estimate of the filter length. This is affirmed by the plot in Fig. 5 that corresponds to modes whose coupling efficiency with the input field is $> 0.01\%$ instead of 0.1%, which shows a better match with the BPM results for $R > 35$dB. The small kink in the red curve appears to be a numerical artifact of the BPM method but the overall trend is as expected. The linear dependence of the filter length beyond $R \sim 35$dB suggest that the curve is dominated by the loss of one/few mode(s) only. Further study revealed that the slope corresponded to the mode that exhibited the lowest loss of 33dB/m and had a coupling efficiency of 0.09%. This mode was excluded from the model when we considered modes with coupling efficiency $> 0.1\%$, but was included for the case $\eta > 0.01\%$. The strong influence of this mode on the filter length illustrates that for long fiber lengths, the modes that have the lowest losses along with a finite coupling efficiency ultimately determine the filtering capability of the fiber. We note that the slope of the curve obtained by the proposed model (when considering modes with $\eta > 0.01\%$) closely follows the slope of the curve obtained through BPM. This suggests that the slight mismatch with the BPM results could be due to the manner in which we have assumed the weighting of the input power (Eq. (4)) into these modes, which essentially represents the ideal case ie. a mode with higher coupling efficiency carries a proportionately larger amount of power. In conclusions, the higher the value of R needed, the larger the number of modes that should be included in the proposed model in order to obtain a correct estimate of the minimum filter length.

4.2. Experimental results

We compared the theoretical estimates of the minimum filter lengths with experimental results obtained in Ref. [14]. A 50cm long fiber was used in these experiments. The mode field radius (a_0) was experimentally found to be $29 \pm 0.4\mu$m, which agrees well with the theoretical value of 29.1μm. In the experiments, a CO_2 laser was focused onto the end facet of the fiber and the output was measured on a CCD camera for various fiber lengths. Single mode output was obtained for a length of ≈ 50cm. This was significantly longer than the 12cm predicted using the previous model. In contrast, we predict a length of 26cm using our revised model to achieve a contrast of 30dB (the maximum obtainable in the experiments due to the limited dynamic range of the camera and background noise level) which is again significantly shorter than the observed length but better than the previous estimates. The discrepancy in Ref. [14] is attributed to mode coupling in the fiber, which is not accounted for by our model and could serve to drastically increase the length needed. Given the experimental difficulties and uncertainties, we consider the comparison of our model with experiment to be encouraging.

4.3. Effect of spatial filtering at the output

The simulations presented above showed that achieving $R = 40$dB required ≈ 30cm long silver halide fiber. There have been recent reports on silver halide and chalcogenide fibers that suggest that introducing a spatial filter at the output end of the fiber can enhance the filtering

#103283 - $15.00 USD Received 27 Oct 2008; revised 24 Dec 2008; accepted 18 Jan 2009; published 30 Jan 2009

performance [19, 20] and thereby reduce the required fiber length. We explored this possibility and studied the effect of introducing a circular aperture at the fiber output on the value of R with the aim to estimate the aperture radius required to provide the optimal rejection of the cladding modes. The circular aperture was simulated with a numerically simulated circular aperture at the output end of the fiber. Figure 6 shows the effect of varying the aperture size on the filtering capability of two lengths of the silver halide fiber analyzed in the earlier sections. Equation (1) was used to obtain the value of R. The fraction of power in the FM was normalized to the throughput power (local power after the aperture) and it was assumed that the fraction that was not coupled into the FM was carried by the cladding modes. It can be seen that R increases almost exponentially as the aperture size is reduced below the mode field radius, a_0. This is because most of the cladding modes extend well into the cladding and get cut-off by the aperture, thereby decreasing the cladding modal content and improving the filtering performance. However, reducing the aperture size would not increase R infinitely because of the presence of cladding modes that have maxima in the center of the fiber core (as shown in Fig. 2). Introduction of the aperture also reduces the throughput power drastically and it drops well below 90% even when the radius of the aperture is equal to a_0. For a fiber length of 50cm and aperture radius of 30μm, the throughput is only 86%. For $2a_0 <$ aperture radius $< 5a_0$, the rate of decrease in R becomes slower while throughput in the FM is $\sim$ 99.99%. The optimum radius of the aperture lies within this range and increases the value of R by at least $5-10$dB, and provides $>$ 99.99% power transmission for the FM. For eg. an aperture radius of 100μm provides the maximum rejection ratio of 52.6dB and throughput of 99.99% for a fiber length of 50cm. In comparison, the aperture radius should be around 300μm to obtain a throughput of 99.999 %, which yields a lower rejection ratio of 46.55dB. For aperture sizes greater than $5a_0$, the spatial filtering has negligible effect. It should also be noted that introduction of the aperture would reduce the broadband filtering capability of the fiber. Thus, there exits a trade-off among the filtering capability of the fiber, the maximal throughput power and the broadband wavelength range that can be achieved.

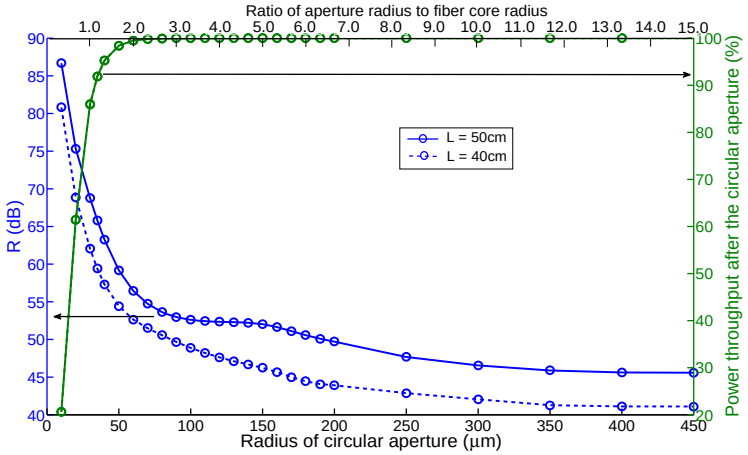

Fig. 6. The effect of varying the radius of a circular aperture placed at the output end of the single-mode fiber. There exits a trade-off between improving the filtering capability and obtaining maximal throughput power. Note that the power throughput does not change significantly for the two fiber lengths.

#103283 - $15.00 USD Received 27 Oct 2008; revised 24 Dec 2008; accepted 18 Jan 2009; published 30 Jan 2009

4.4. *Bulk/boundary scattering effects*

Silver halide fibers are poly-crystalline in nature and scattering (bulk/boundary) of the modes is an important aspect that affects their filtering capability. Scattering of a guided mode into radiation modes is a stochastic problem, which results in transfer of power from the FM to the cladding modes and manifests itself as radiation loss of the FM. Published reports indicate that the radiation loss (due to boundary scattering) itself is independent of the nature of the roughness distribution [21, 22]. For boundary roughness such that the variance in roughness $<< 1$ and a refractive index ratio across the boundary ~ 0.001, the scattering loss of the FM is approximately a few dB/km [22]. Bulk roughness scattering further increases the loss of the FM as well as the cladding modes. The total confinement loss of the FM would be the sum of the scattering loss and the absorption loss. Thus, the effect of the scattering loss would be to increase the loss of the FM by a certain multiplicative factor, which would (ideally) be constant for different fiber sections as long as they are fabricated using the same process and material. This implies that the scattering effects should not affect the minimum filter length for different sections of the same fiber. However, an offset launch can excite different groups of low-loss cladding modes, and depending on the group of modes that are excited by the input field, the minimum filter length may be slightly altered. It should also be noted that since scattering increases the loss of the FM, it would ultimately limit the maximum rejection ratio that can be achieved with these fibers. The scattering amongst the lossy cladding modes is more likely to scatter power from low loss cladding modes into high loss cladding modes (since the latter are more numerous than the former) and hence it is likely to improve matters. Hence by ignoring it, we get a slightly longer estimate of the minimum fiber length, thereby providing a better rejection ratio.

5. Conclusion

Estimating the minimum length of fiber required to achieve wavefront filtering is crucial in stellar interferometry. We have presented a theoretical model that can be applied to estimate the length of the fiber with any arbitrary fiber geometry, including fibers that have a high-index metal coating as the absorption layer. The proposed method provides a more accurate estimate of the minimum filter length than the previously reported models based on considering the loss of LP_{11} mode alone. We show that by considering the loss as well as the coupling efficiency of the cladding modes, we can identify a finite and small number of cladding modes that can provide a better estimate of the minimum filter length. We also show the impact of the launch conditions on the filtering performance of the fiber. Simulations indicate that under ideal launching conditions (Airy disk), symmetric cladding modes that have an intensity maxima at the center of the fiber ultimately determine the filter length. The theoretical estimates of the fiber length obtained through the proposed method show good agreement with numerical results obtained through BPM and experimental observations on silver halide fibers. However, it is important to note that implementing the BPM technique can become very time-consuming for simulating long fiber lengths. Besides, it is inherently unsuitable for studying high-index metal-coated chalcogenide fibers an approach favored by a number of groups. The proposed method does not have these limitations, although the number of modes that need to be considered can become significant for $R > 35$dB. In a practical system the launch is never likely to perfect and so the actual weightings of the launched modes will vary in time and will not match those given here. The main effect of an off-centered launch will be a reduction of the power in the fundamental mode and increase in power in the cladding modes leading to an initial reduction in the rejection ratio. The losses of the fiber modes would remain unaltered. This is understood more clearly by studying Fig. 1. An off-centered launch would reduce the power launched into the FM at the input, thereby pulling down the red curve along the y-axis. The power coupled at

#103283 - $15.00 USD Received 27 Oct 2008; revised 24 Dec 2008; accepted 18 Jan 2009; published 30 Jan 2009

the input into the other leaky cladding modes would also get altered such that they would have, in general, more power coupled into them thereby pushing up the curves along the y-axis. There would be other modes also coming into picture which would correspond to the anti-symmetric modes. But, these modes would also have losses comparable to those of the symmetric modes that have been represented in Fig. 1. Thus, in order to achieve the same rejection ratio of 10^6 the vertical black line now would need to be pushed towards longer fiber length yielding a slightly longer filter length. However, due to the exponential nature of the loss of all the modes and the fact that the order of loss of the symmetric and anti-symmetric cladding modes are similar, any increase in the total fiber length required will be small as compared to the minimum length obtained for an on-axis launch.

We have also presented theoretical simulations that show that by incorporating an optimum circular aperture at the output, the filtering performance of the fiber can be improved by at least $5-10$dB without compromising the throughput power, thereby reducing the minimum fiber length significantly. The results suggest that the excitation/launching conditions are crucial in achieving optimum performance of the wavefront filter in any practical setup.

Acknowledgments

This work was supported in part by the European Space Agency under contracts 17005/02/NL/JA and 20914/07/NL/CP. The authors would also like to thank L. K. Cheng and W.L.M. Gielesen (TNO Science and Industry, Netherlands) for useful discussions on the chalcogenide fibers.

#103283 - $15.00 USD Received 27 Oct 2008; revised 24 Dec 2008; accepted 18 Jan 2009; published 30 Jan 2009